Quenching of Growth of ZnO Nanoparticles by Adsorption of Octanethiol

ARTICLE *in* THE JOURNAL OF PHYSICAL CHEMISTRY B · JUNE 2002

Impact Factor: 3.3 · DOI: 10.1021/jp0144606

4 AUTHORS, INCLUDING:

Peter Searson
Johns Hopkins University
297 PUBLICATIONS **11,668** CITATIONS

SEE PROFILE

Quenching of Growth of ZnO Nanoparticles by Adsorption of Octanethiol

Noshir S. Pesika,[†] Zeshan Hu,[‡] Kathleen J. Stebe,[†] and Peter C. Searson*[,‡]

Department of Chemical Engineering and Department of Materials Science & Engineering, Johns Hopkins University, Baltimore, Maryland 21218

Received: December 10, 2001; In Final Form: May 6, 2002

To exploit the size dependent properties of nanoparticles, it is essential to control the particle size. We show that injection of octanethiol into suspensions of ZnO particles can be used to quench particle growth. X-ray photoelectron spectroscopy studies of the adsorption of octanethiol on ZnO single crystals indicate relatively weak adsorption of thiolate and sulfonate species dependent on the crystal orientation. These results suggest that adsorption of thiolate and sulfonate groups on ZnO particles in suspension prevent dissolution of the solid phase. Furthermore, the octanethiol is adsorbed sufficiently strongly to quench growth but can be easily removed for subsequent surface functionalization.

Introduction

When the size of a particle is less than a characteristic length scale of interest, such as the diameter of an exciton or the mean free path of an electron, then the properties of the particle can be significantly different from the bulk material. Such particles can be used as individual elements in a wide range of devices or can be assembled into larger scale structures. To exploit the size-dependent properties of particles for specific applications, it is essential to develop synthesis techniques that allow control of particle size.

A wide range of metal and semiconductor nanoparticles have been produced by synthesis from homogeneous solution.[1−4] Microemulsion-mediated synthesis has been exploited to grow nanoparticles with sharp size distributions. The particle diameters that can be obtained using this technique are determined by the size of the micelles in the microemulsion.[5] Nanoparticles have also been synthesized from solution containing capping molecules so that, upon nucleation, the particles are immediately capped by the surfactant and there is no subsequent growth.[6,7] In another approach, the solvent for the reaction itself can act as a capping agent; for example, *n*-trioctylphosphine (TOPO) has been used to arrest the growth of CdSe nanoparticles[8] at diameters between 0.9 and 3 nm. Once again, growth is quenched immediately after nucleation of the particles. Another strategy for obtaining nanoparticles using solution phase synthesis is to allow the particles to grow to a specific size and then to quench growth by the injection of a suitable capping molecule.

In previous work,[9] we have shown that the growth of ZnO nanoparticles in solution phase synthesis can be arrested by injection of a suitable capping ligand. In this paper, we report on the role of octanethiol in quenching the growth of ZnO nanoparticles in suspension. ZnO single crystals are used as a model system to study the adsorption process. We show that octanethiol adsorbs onto ZnO and that the nature of the interaction is dependent on the crystal orientation. Octanethiol primarily adsorbs as a thiolate on the $(000\bar{1})$O surface, and is adsorbed primarily as an oxidized species of the thiol (e.g., sulfonate) on the (0001)Zn surface.

Experimental Section

Materials. Premium (I) grade zinc oxide single crystals, with either (0001)Zn or $(000\bar{1})$O surfaces, were purchased from Eagle Pitcher. All reagents were purchased from Aldrich, including reagent grade $Zn(CH_3CO_2)_2 \cdot 2H_2O$, conductivity grade NaOH, and octanethiol (98.5% purity), HPLC grade solvents for use in the X-ray photoelectron spectroscopy studies (2-propanol, methanol, and ethanol) and ACS grade 2-propanol for use in the nanoparticle growth and quenching experiments. All glassware was soaked in 18 M sulfuric acid overnight and rinsed with purified water. Water was distilled and deionized using a Millipore Milli-Q 50 Purification System (Bedford, MA) which had a resistivity of not less than 18.0 MΩ cm. In all of the experiments, the chemicals were used as received.

Particle Synthesis. ZnO nanoparticles were synthesized by precipitation from 2-propanol.[10,11] The nucleation reaction can be written as

$$Zn(CH_3CO_2)_2 + 2NaOH \rightarrow ZnO + H_2O + 2NaCH_3CO_2$$

For a typical synthesis, 1.0 mmol of zinc acetate dihydrate was dissolved in 80.0 mL 2-propanol under constant stirring at 50 °C. A 0.02 M solution of NaOH in 2-propanol was prepared by adding approximately 0.08 g of NaOH to 2-propanol under constant stirring at 50 °C. For a typical reaction, 8.0 mL of the zinc acetate solution was diluted to 92 mL with 2-propanol. The reaction flask was then placed in a water bath at 65 °C. Thereafter, 8.0 mL of the NaOH solution was rapidly added to the reaction flask (within 3 s) with the temperature maintained at 65 ± 2 °C. The reaction flask was isolated from the surroundings using a venting tube immersed in 2-propanol. The reaction flask remained sealed except for brief intervals (less than 10 s) during which aliquots were removed for subsequent analysis.

* To whom correspondence should be addressed.
[†] Department of Chemical Engineering, Johns Hopkins University.
[‡] Department of Materials Science & Engineering, Johns Hopkins University.

10.1021/jp0144606 CCC: $22.00
Published on Web 06/18/2002

Transmission electron microscopy and X-ray diffraction studies have shown that the particles are single crystals with the characteristic zincite structure.[9,11]

Preparation of Octanethiol Solution. A stock solution of the capping agent was prepared by adding 0.15 mL octanethiol to 100 mL of 2-propanol. This solution was added in varying amounts to the stirred reaction solution after the reaction had proceeded for 15 min. The concentration of the octanethiol in the reaction flask ranged from 0 to 0.177 mM. Thereafter, the reaction was allowed to proceed for 4 h, during which aliquots were removed for analysis.

Determination of Water Concentration. At the end of the growth and capping experiments, a 1.0 mL sample of the reaction solution was withdrawn for determination of the concentration of water using a Metrohm 684 KF coulometer. The concentration of water in all experiments ranged from 27.5 mM to 35.3 mM.

UV Spectroscopy. Absorption spectra were recorded using a Shimadzu UV-2101PC scanning spectrophotometer. Three-mL aliquots were withdrawn from the reaction solution at predetermined intervals. To quench any further reaction, the samples were immediately placed in ice water and stored under ice until the spectra were obtained, usually within 15 min. Pure 2-propanol was used as the reference. Standard quartz cells (Fisher) with a 10 mm path-length were used and rinsed with 2-propanol after each run.

X-ray Photoelectron Spectroscopy. X-ray photoelectron spectroscopy experiments were carried out with a Phi 5100 spectrometer using a Mg K_α (1253.6 eV) source to study the adsorption of octanethiol on ZnO (0001) single crystals. Experiments were performed on both the (0001)Zn and $(000\bar{1})$O polar surfaces at a 45° takeoff angle. The samples were introduced and analyzed in a UHV chamber ($P_{base} < 2 \times 10^{-8}$ Torr) equipped with a fast entry load-lock cell. All spectra were referenced to the Zn ($2p_{3/2}$) peak at 1021.7 eV. Prior to each experiment, the ZnO single crystals were rinsed in 2-propanol. The crystals were then immersed for 24 h in a solution containing 3.0 mM octanethiol in 2-propanol. Spectra were obtained for both the (0001)Zn and $(000\bar{1})$O surfaces under the following conditions: (i) as-received crystals rinsed in 2-propanol, (ii) after immersion in octanethiol, (iii) after immersion in octanethiol followed by rinsing in 2-propanol, and (iv) after immersion in octanethiol followed by rinsing in 2-propanol followed by water.

Contact Angle Measurements. Contact angle measurements were taken using a goniometer (Rame-Hart model 100−00115) under ambient conditions. The crystals were cleaned by sonication in water for 10 min followed by sonication in 2-propanol for 5 min, rinsing with 2-propanol, and finally dried in air. The crystals were then immersed in a 3 mM solution of octanethiol for 24 h, and either used directly or subjected to rinsing prior to use. A micropipet was used to deliver a 10.0 μL sessile drop of water. Measurements were taken at two different locations on the crystals and the average is reported.

Results and Discussion

Growth of ZnO Nanoparticles. Figure 1a shows absorbance spectra for the synthesis of ZnO nanoparticles in the absence of any capping molecule. The spectra all show a well-defined exciton peak characteristic of solid ZnO immediately after mixing the zinc acetate and sodium hydroxide solutions, indicating that nucleation is fast. The absorption onset red-shifts with time showing that the average particle size is in the quantum regime. The average particle size can be determined

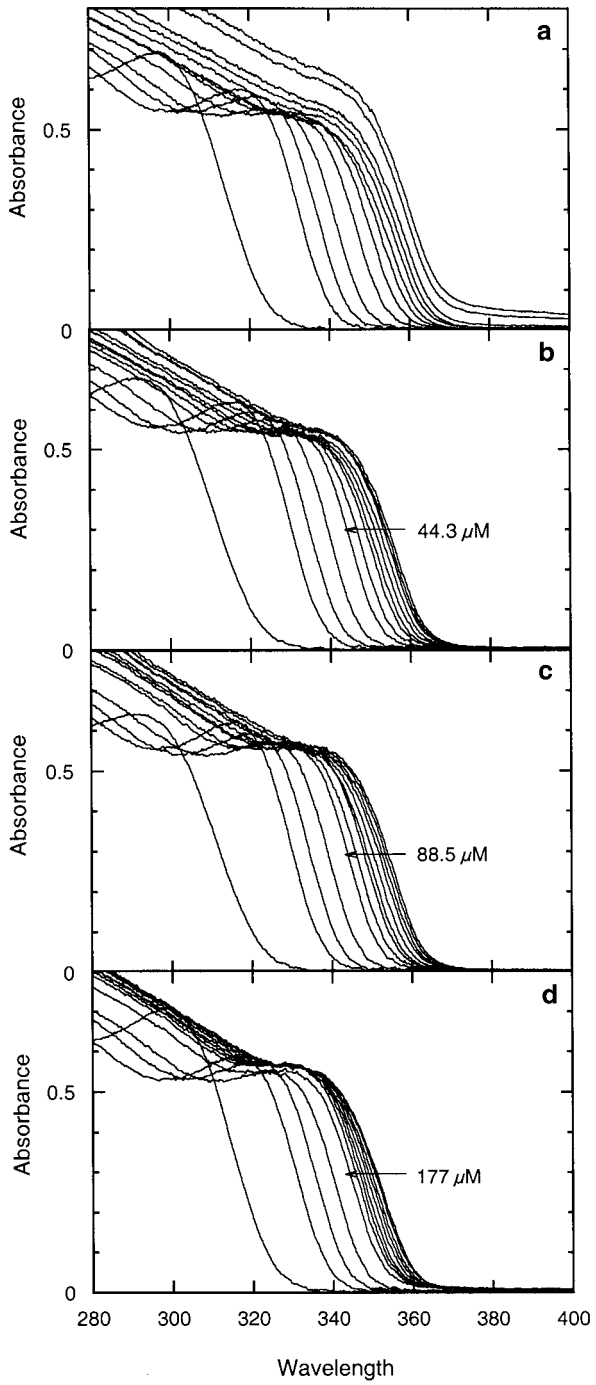

Figure 1. (a)−(d) Absorbance spectra for synthesis of zinc oxide nanoparticles from $Zn(CH_3CO_2)_2$ in 2-propanol at 65 °C for 4 h after 0, 2, 4, 8, 18, 30, 60, 90, 120, 150, 180, 210, and 240 min. The arrows indicate the injection of (b) 44.3 μM, (c) 88.5 μM, and (d) 177 μM octanethiol after 15 min.

from the effective mass model[12,13]

$$E^* \cong E_g^{\text{bulk}} + \frac{\hbar^2\pi^2}{2er^2}\left(\frac{1}{m_e m_o} + \frac{1}{m_h m_o}\right) - \frac{1.8e}{4\pi\epsilon\epsilon_o r} - \frac{0.124e^3}{\hbar^2(4\pi\epsilon\epsilon_o)^2}\left(\frac{1}{m_e m_o} + \frac{1}{m_h m_o}\right)^{-1} \quad (1)$$

where E^* is the band gap in eV, E_g^{bulk} is the bulk band gap, r is the particle radius, m_e is the effective mass of the electrons, m_h is the effective mass of the holes, m_o is the mass of a free

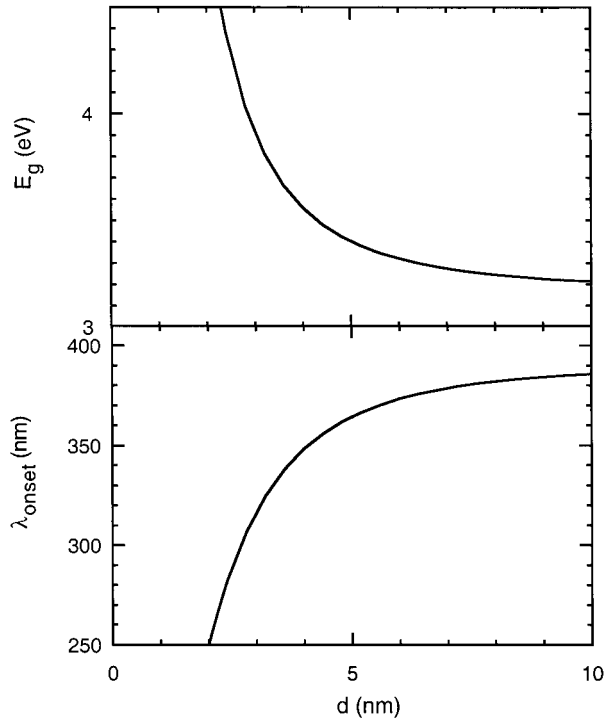

Figure 2. Band gap and absorbance onset versus particle diameter for ZnO.

electron, ϵ is the relative permittivity, ϵ_o is the permittivity of free space, $\hbar$ is Planck's constant, and e is the charge on the electron.

Because the effective masses for electrons and holes in ZnO are relatively small ($m_e = 0.26$, $m_h = 0.59$), band gap enlargement can be seen for particle diameters less than about 8 nm. The absorption onset immediately after nucleation is about 320 nm, corresponding to an average particle diameter of 3 nm. Further growth of the particle causes a decrease in the band gap and hence a red shift of the absorption onset. For particle diameters larger than about 8 nm, the absorption onset would be expected to saturate at about 388 nm corresponding to the bulk band gap for ZnO. Figure 2 shows the band gap and the corresponding absorbance onset plotted as a function of particle radius as predicted by eq 1 with $m_e = 0.26$, $m_h = 0.59$, $\epsilon = 8.5$, and $E_g^{bulk} = 3.2$ eV.[14−16] The validity of this approach was confirmed from analysis of high-resolution transmission electron microscopy (HRTEM).[11]

The evolution of the particle radius with time is presented in Figure 3. In solution phase synthesis, processes such as coarsening and aggregation can compete with nucleation and growth in modifying the particle size distribution in the system. According to the Lifshitz−Slyozov−Wagner model,[17,18] the rate law for coarsening is given by

$$\bar{r}^3 - \bar{r}_o^{\,3} = kt \qquad (2)$$

where $\bar{r}$ is the average particle radius, $\bar{r}_o$ is the initial particle radius, t is time, and k is the rate constant. The rate constant is dependent on the molar volume of the solid phase, the surface energy, the bulk solubility, and the diffusion coefficient for metal ions in solution. Figure 4 shows the time dependence of the particle size replotted as r^3 versus time. After about 30 min, the linear region shows that at longer times the increase in particle size is determined solely by diffusion-limited coarsening, according to equation 2, where larger particles grow at the expense of smaller particles. Furthermore, these results indicate

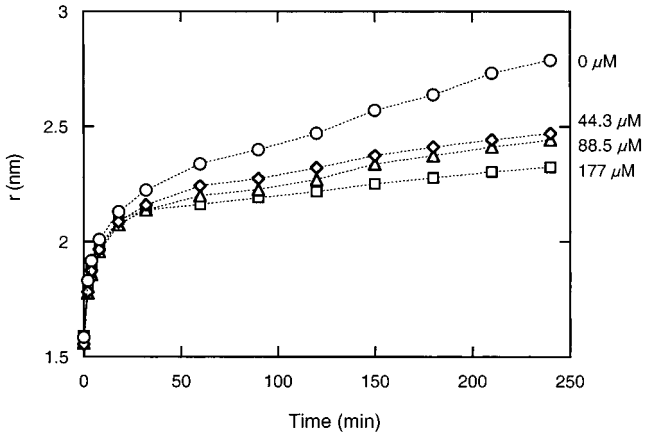

Figure 3. Particle radius versus time for growth of ZnO nanoparticles at 65 °C with the injection of 0, 44.3 μM, 88.5 μM, and 177 μM octanethiol after 15 min.

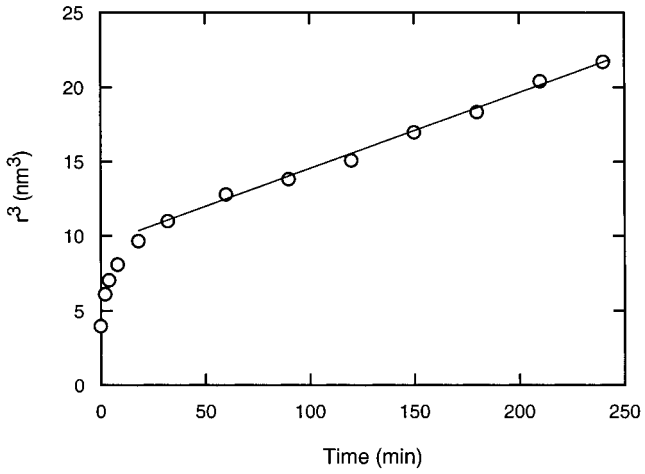

Figure 4. Particle radius cubed versus time for growth of ZnO nanoparticles at 65 °C.

that the supersaturation is depleted, and hence growth is completed, after about 30 min. From the slope of the linear region we obtain a value for the coarsening rate constant k of 8.7×10^{-4} nm^3 s^{-1}.

We note that at the end of each experiment, the concentration of water was in the range of 27.5 mM to 35.3 mM. The concentration of water in 2-propanol prior to preparing solutions for each experiment was typically about 3 mM and the crystal water associated with the zinc acetate dihydrate corresponds to 2 mM. In addition, 1 mM water is produced from the synthesis. Thus, most of the water in the solution is absorbed from the atmosphere during the preparation of the solutions. Transparent suspensions were obtained only if the water concentration was higher than about 20 mM. At lower water concentrations, the suspensions were translucent and the absorption spectra exhibited significant background absorbance. This result suggests that water is necessary to provide sufficient surface charge to prevent aggregation. Experiments with different capping molecule concentrations were performed at the same time in order to minimize differences in the concentration of water.

Capping with Octanethiol. In Figure 1, parts b−d, absorbance spectra are presented for ZnO suspensions to which 44.3, 88.5, or 177 μM octanethiol was injected after 15 min. The absorbance spectra show an immediate retardation in particle growth after injection of the surfactant, as apparent in the slower red-shift of the absorbance onset. Figure 3 shows the particle size versus time with the injection of different concentrations

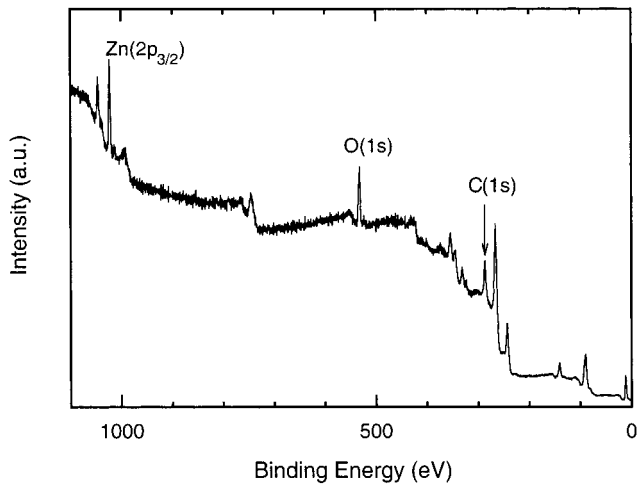

Figure 5. X-ray photoelectron spectroscopy survey scan of the polar (0001)Zn surface of a ZnO single crystal.

of octanethiol, illustrating that rate of increase in particle size decreases with increasing octanethiol concentrations.

The addition of 177 μM octanethiol corresponds to monolayer coverage on particles with 2.5 nm radius assuming that all Zn is reacted to form ZnO, and that octanethiol has a headgroup area of 16 Å^2.[19] From the molar volume of ZnO (14.3 cm^3 mole^{-1}), the particle density for a particle radius of 2.5 nm is 2.19×10^{-14} cm^{-3} corresponding to a total ZnO surface area of 1.72×10^{-21} Å^2 L^{-1}. This calculation assumes that all of the surfactant is adsorbed on the particles. Partitioning of the surfactant to the bulk solution and to the liquid/gas interface is expected to lower surface coverage on the particles. This effect may be responsible for the fact that the particle growth is not completely arrested with injection of 177 μM octanethiol.

Surface Characterization. The decrease in growth rate associated with increasing concentration suggests that the octanethiol is adsorbed on the surface thereby slowing particle growth. Hydroxamic acids, alkylphosphonic acids, and carboxylic acids are known to form self-assembled monolayers on many metal oxides.[20−22] Alkanethiols form self-assembled monolayers on copper oxide[23] and silver oxide,[22] however, to our knowledge there are no reports of thiol adsorption on ZnO. Recently, thiols have been shown to adsorb on ZnSe[24] although ordered self-assembled monolayers were only obtained for relatively long chain lengths (pentadecanethiol). To obtain more insight into the mechanism of quenching, the adsorption of octanethiol on the (0001) surfaces of ZnO single crystals was studied using XPS. Zinc oxide has a wurtzite crystal structure so that the (0001) surfaces are either zinc terminated (the (0001)-Zn surface) or oxygen terminated (the (000$\bar{1}$)O surface).

TABLE 1: Peak Assignments for XPS Spectra[24]

peak position (eV)	peak assignment
1046	Zn $2p_{1/2}$
1022	Zn $2p_{3/2}$
761	O KL_1L_{23}
744	O $KL_{23}L_{23}$
532	O 1s
424	Zn $L_3M_{23}M_{23}$
353	Zn $L_3M_{23}M_{45}$ (^{1}P)
344	Zn $L_3M_{23}M_{45}$ (^{3}P)
330	Zn $L_2M_{23}M_{45}$ (^{1}P)
285	C 1s
265	Zn $L_3M_{45}M_{45}$
242	Zn $L_2M_{45}M_{45}$
140	Zn 3s
89	Zn 3p
11	Zn 3d

Figure 5 shows a survey scan for the (0001)Zn surface of a ZnO single crystal. Peaks corresponding to Zn and O, along with their corresponding auger peaks are clearly evident. Table 1 lists the peak assignments along with their corresponding binding energies.[24]

The Zn ($2p_{3/2}$), O (1s), and C (1s) spectral regions are shown in Figure 6. The Zn ($2p_{3/2}$) peak is characteristic of Zn^{2+}, and is the same for both the (0001)Zn and (000$\bar{1}$)O surfaces. We note that the escape depth of the photoelectrons at a 45° take off angle corresponds to about four monolayers or two Zn/O bilayers. The C (1s) peak at 285 eV is caused by surface contamination and is also the same for both faces. The O (1s) spectrum consists of two peaks related to O^{2-} in the ZnO lattice (530.5 eV) and surface hydroxyl groups (532 eV).[25,26]

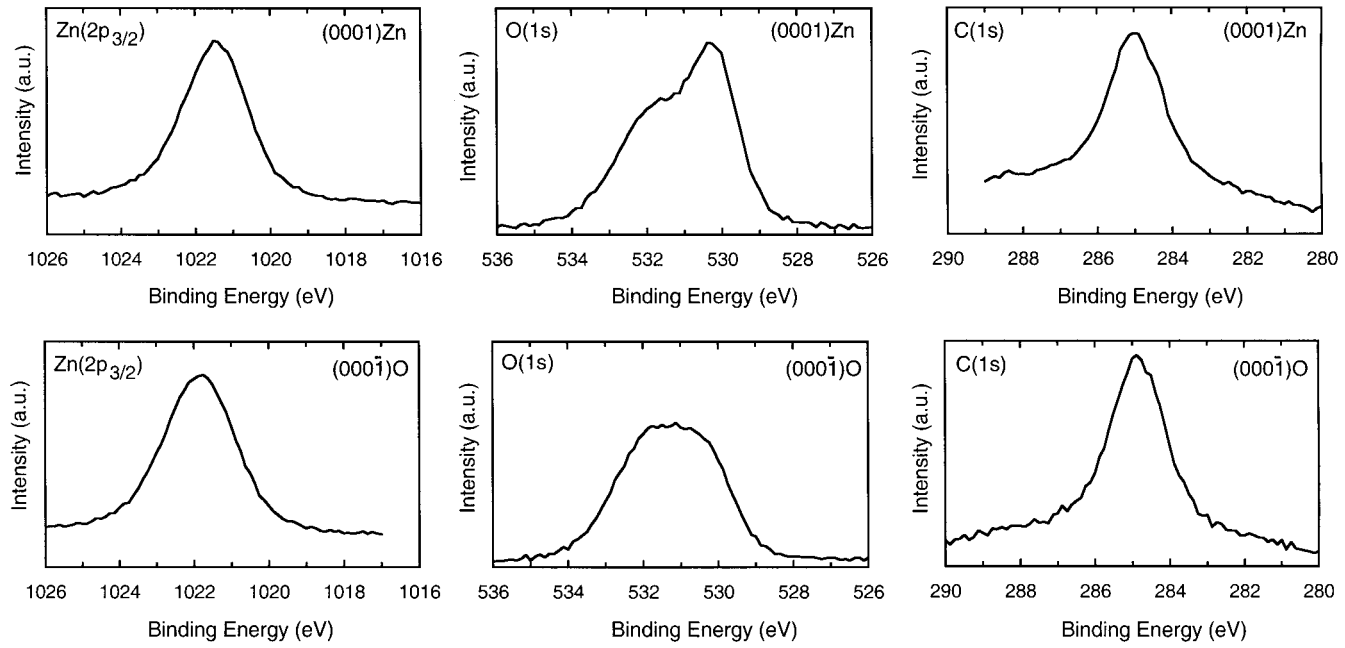

Figure 6. X-ray photoelectron spectra of (0001)Zn and (000$\bar{1}$)O surface of ZnO single crystals showing the Zn ($2p_{3/2}$), O (1s), and C (1s) regions.

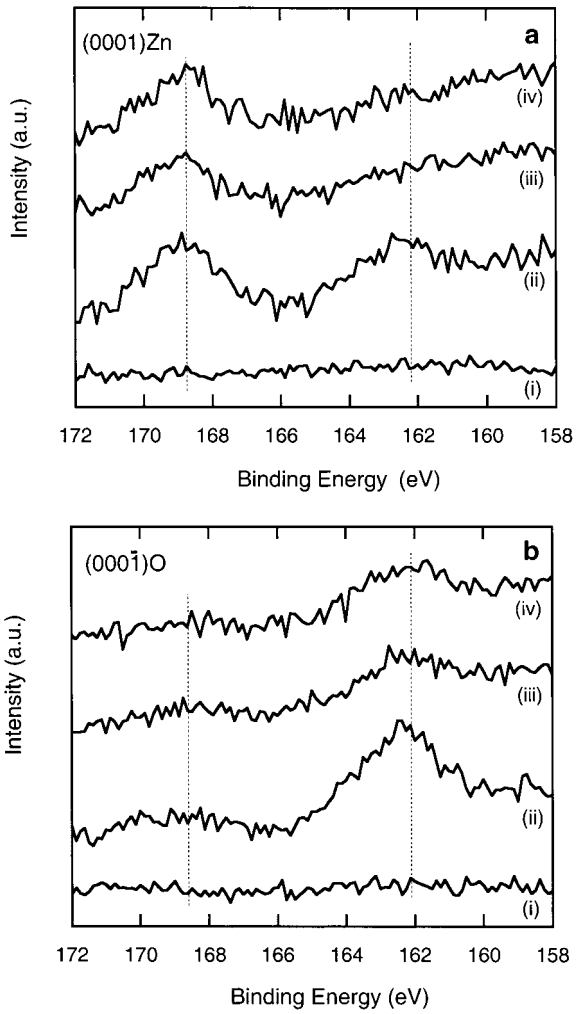

Figure 7. X-ray photoelectron spectra for the S (2p) region of the (a) (0001)Zn surface, and (b) the (000$\bar{1}$)O surface of ZnO single crystals; (i) no thiol, (ii) immersion in octanethiol without subsequent rinsing, (iii) immersion in octanethiol followed by rinsing in 2-propanol, and (iv) immersion in octanethiol followed by rinsing in 2-propanol and then water. Spectra are shifted along the vertical axis for convenience.

Figures 7a and b show the sulfur region of the spectrum for the (0001)Zn and (000$\bar{1}$)O surfaces, respectively. The lowermost scan ((i) in Figure 7) shows the sulfur region for both faces without exposure to octanethiol. The scan above it ((ii) in Figure 7) shows the spectra for crystals after immersion in octanethiol solution. These samples were not rinsed with solvent before scanning. Both faces show well-defined thiolate peaks at 162.1 eV characteristic of thiol adsorption at the surface.[27] The (0001)-Zn surface shows an additional sulfonate peak at 168.5 eV due to an oxidized form of the thiol (e.g., $R-SO_3^-$, $R-SO_4^-$). Oxidation of the thiol has been reported for self-assembled monolayers on gold and is associated with UV exposure and the slow reaction with the oxygen in the atmosphere.[27,28] The thiolate peak on the (000$\bar{1}$)O surface is much stronger than the thiolate peak on the (0001)Zn surface, indicating that the thiolate species is more stable on the (000$\bar{1}$)O surface.

In the gas phase, the (0001)Zn surface is known to be more reactive than the (000$\bar{1}$)O surface. For example, methanol, ethanol, propanol, acetic acid, and acetone adsorb dissociatively on the (0001)Zn surface but only adsorb in the molecular form on the (000$\bar{1}$)O surface.[29−31] Water is known to adsorb more strongly on the (0001)Zn surface than on the (000$\bar{1}$)O surface.[32] Thus, oxidation of the thiol on the (0001)Zn surface is consistent with the catalytic activity of this surface.

TABLE 2: Static Contact Angle Measurements (10 μL drop size)

condition	contact angle (deg) (0001)Zn surface	contact angle (deg) (000$\bar{1}$)O surface
no thiol	29 ± 2	33 ± 2
octanethiol, no rinse	74 ± 2	71 ± 2
octanethiol, 2-propanol rinse	66 ± 2	47 ± 2
octanethiol, 2-propanol & water rinse	48 ± 2	40 ± 3

After immersion in octanethiol solution and rinsing in 2-propanol ((iii) in Figure 7) the (000$\bar{1}$)O surface still shows a strong thiolate peak and a very small sulfonate peak. The small decrease in intensity of the thiol peak on rinsing implies a slight decrease in surface coverage due to weak adsorption. The thiolate peak on the (0001)Zn surface is no longer present after rinsing in 2-propanol suggesting that the thiolate species is very weakly bound to the (0001)Zn surface.

Finally, the uppermost spectra ((iv) in Figure 7) correspond to crystals which were immersed in octanethiol solution and rinsed with 2-propanol and subsequently with water. These spectra clearly show a well-defined thiolate peak on the (000$\bar{1}$)O surface and a well-defined sulfonate peak on the (0001)Zn surface. These results further show preferential adsorption of thiolate on the (000$\bar{1}$)O surface and sulfonate on the (0001)Zn surface and suggest that the attenuation of the growth kinetics of the ZnO nanoparticles is due to the formation of weakly adsorbed thiolate and sulfonate species at the surface.

Contact angle measurements obtained for both the (0001)Zn and (000$\bar{1}$)O surfaces of ZnO single crystals are summarized in Table 2. For a typical contact angle measurement, the crystal was removed from the octanethiol solution and allowed to air-dry for approximately 2 min. The as-received crystals, after rinsing in methanol, ethanol, and water are relatively hydrophilic with contact angles ranging from 29°−33° for either face. The increase in the contact angle after immersion in octanethiol solution is indicative of adsorption with the hydrophobic tails exposed. After rinsing in 2-propanol, the contact angle decreases on both the (0001)Zn and (000$\bar{1}$)O surfaces. The S (2p) XPS spectrum for the (000$\bar{1}$)O surface showed a slight decrease in the magnitude of the dominant thiolate peak after rinsing in 2-propanol, suggesting a decrease in coverage, consistent with the decrease in contact angle. The S (2p) spectrum for the (0001)Zn surface showed no thiolate peak but a significant sulfonate peak after rinsing in 2-propanol. The relatively small decrease in contact angle indicates that the sulfonate linkage is relatively stable in 2-propanol. After rinsing in 2-propanol and subsequently in water, the contact angle decreases further, suggesting a further decrease in the coverage of the thiolate and sulfonate at the surface. Note that the decrease in the contact angle is larger for the (0001)Zn surface suggesting that the sulfonate is the more soluble in water than the thiolate.

Although the adsorption of thiol onto ZnO is clearly not as strong as on a gold surface, the interaction is sufficiently strong to quench nanoparticle growth. Thiol adsorption provides a barrier that prevents dissolution of the particles and hence arrests further growth.

Conclusions

Octanethiol is confirmed to quench the growth of ZnO nanoparticles. XPS and contact angle measurements indicated that octanethiol adsorbs reversibly to ZnO single crystals primarily as a thiolate species on the (000$\bar{1}$)O surface and a

sulfonate on the (0001)Zn surface. The results from the quenching experiments indicate that octanethiol adsorbs onto the facets of the ZnO nanocrystals. The octanethiol is adsorbed sufficiently strongly to quench growth but can be easily removed for subsequent surface functionalization.

Acknowledgment. This work was supported by the JHU MRSEC (NSF Grant No. DMR00-80031). N.S.P gratefully acknowledges support through a NASA graduate fellowship.

References and Notes

(1) Henglein, A. *Top. Curr. Chem.* **1988**, *143*, 113.
(2) Matijevic, E. *Langmuir* **1986**, *2*, 12.
(3) Steigerwald, M. L.; Brus, L. E. *Acc. Chem. Res.* **1990**, *23*, 183.
(4) Murray, C. B.; Kagan, C. R.; Bawendi, M. G. *Annu. Rev. Mater. Sci.* **2000**, *30*, 545.
(5) Hingorani, S.; Pillai, V.; Multani, M. S.; Shah, D. O. *Mater. Res. Bull.* **1993**, *28*(12), 1303.
(6) Nosaka, Y.; Ohta, N.; Fukuyama, T.; Fujii, N. *J. Colloid and Int. Sci.* **1992**, *155*, 23.
(7) Mahamuni, S.; Khosravi, A. A.; Kundu, M.; Kshirsagar, A. *J. Applied Phys.* **1993**, *73*, 5237.
(8) Katari, J. E.; Colvin, V. L.; Alivisatos, A. P. *J. Phys. Chem.* **1994**, *98*, 1409.
(9) Wong, E. M.; Hoertz, P. G.; Liang, C. J.; Shi, B.; Meyer, G.; Searson, P. C. *Langmuir*, submitted.
(10) Bahmenann, D. W.; Kormann, C.; Hoffmann, M. R. *J. Phys. Chem.* **1987**, *91*, 3789.
(11) Wong, E. M.; Bonevich J. E.; Searson, P. C. *J. Phys. Chem.* **1998**, *102*, 7770.
(12) Schmid, G.; Chi, L. F. *Adv. Mater.* **1998**, *10*(7), 515.
(13) Brus, L. *J. Phys. Chem.* **1983**, *79*, 5566.
(14) S. Shionoya In *Phosphor Handbook*; Shionoya, S.; Yen, W. M., Eds.; CRC: Boca Raton, FL, 1998.
(15) Berger, L. I. *Semiconductor Materials*; CRC: Boca Raton, FL, 1997; p.184.
(16) Sze, *Physics of Semiconductor Devices*; Wiley: New York 1981 p 849.
(17) Liftshitz, I. M.; Slyozov, V. V. *J. Phys. Chem. Solids* **1961**, *19*, 35.
(18) Wagner, C. *Z. fur Elecktrochemie* **1961**, *65*, 581.
(19) Korgel, B. A.; Fullam, S.; Connolly, S.; Fitzmaurice, D. *J. Phys. Chem. B* **1998**, *102*, 8379.
(20) Goetting, L. B.; Deng, T.; Whitesides, G. M. *Langmuir* **1999**, *15*, 32.
(21) Laibinis, P. E.; Hickman, J. J.; Wrighton, M. S.; Whitesides, G. M. *Science* **1989**, *245*, 845.
(22) Folkers, J. P.; Gorman, C. B.; Laibinis, P. E.; Buchholz, S.; Whitesides, G. M.; Nuzzo, R. G. *Langmuir* **1995**, *11*, 813.
(23) Sung, M. M.; K.; Kim, C. G.; Lee, S. S., Kim, Y. *J. Phys. Chem.* **2000**, *104*, 2273.
(24) Noble-Luginbulh, A. R.; Nuzzo, R. G. *Langmuir* **2001**, *17*, 3937.
(25) Mintas, M.; Filby, G. W. *Z. Naturforsch.* **1981**, *36*, 140.
(26) Casarin, M.; Favero, G.; Glisenti, A.; Granozzi, G.; Maccata, C.; Tabacchi, G.; Vittadini, A. *J. Chem. Soc., Faraday Trans.* **1996**, *92*(17), 3247.
(27) Hutt, D. A.; Cooper, E.; Leggett, G. J. *J. Phys. Chem. B* **1998**, *102*, 174.
(28) Rieley, H.; Kendall, G. K.; Zemicael, F. W.; Smith, T. L.; Yang, S. *Langmuir* **1998**, *14*, 5147.
(29) Vohs, J. M.; Barteau, M. A. *Surf. Sci.* **1988**, *201*, 481.
(30) Vohs, J. M.; Barteau, M. A. *Surf. Sci.* **1989**, *221*, 590.
(31) Vohs, J. M.; Barteau, M. A. *J. Phys. Chem.* **1991**, *95*, 297.
(32) Zwicker, G.; Jacobi, K. *Surf. Sci.* **1983**, *131*, 179.